Desalination and Water Treatment
www.deswater.com

doi: 10.1080/19443994.2014.930799

55 (2015) 1864–1875
August

Taylor & Francis
Taylor & Francis Group

Utilization of synthesized NaA and ZSM-5 nanozeolites for mercury(II) removal: kinetic, thermodynamic and isotherm study

Hassan Alijani[a], Mostafa Hossein Beyki[b], Seyed Nima Mirzababaei[c,*]

[a]*Department of Chemistry, Amirkabir University of Technology, Tehran, Iran*
[b]*School of Chemistry, University College of Science, University of Tehran, Tehran, Iran*
[c]*Faculty of Science, Chemistry Department, University of Guilan, Rasht, Iran, Tel. +98 01912146477; email: shahab.ta20@gmail.com*

Received 11 December 2013; Accepted 20 May 2014

ABSTRACT

In this research, two types of nanozeolite i.e. NaA and ZSM-5 were synthesized and utilized as a sorbent for removal of mercury(II) from aqua's media. The prepared nanosorbents were characterized with scanning electron microscopy, X-ray diffraction and Fourier transformed infrared techniques. Effect of pH, interaction time, temperature and other important parameter for removal of mercury(II) was investigated. The adsorption isotherm models were studied based on Langmuir, Freundlich and Temkin models. The positive values of standard enthalpy of adsorption exhibit the endothermic nature of the adsorption process. The values of Gibbs free energy were negative for ZSM-5 and positive for NaA. But with increasing the temperature, amount of Gibbs energy tends to be more negative therefore, the adsorption can be more effective in higher temperature. Moreover, kinetic investigation revealed that the pseudo-second-order sorption mechanism is predominant. According to experimental results, the ZSM-5 is more efficient for removal of mercury(II) with respect to NaA nanozeolite.

Keywords: Nanozeolite; Mercury; Isotherm; Heavy metal

1. Introduction

Mercury is classified among priority hazardous compounds according to the European Union legislation, as the maximum allowable level for mercury in surface waters is $0.07\,\mu g\,L^{-1}$ hence, its pollution is a global crisis facing society today [1–5]. A wide variety of industries can generate mercury-containing solid wastes or wastewater, including weapons production, copper and zinc smelting, gold mining, painting application, fertilizer industry, mining facilities and tanneries [6–12]. Methyl mercury and forms of mercury with relatively low toxicity can be bioconcentrated in organisms and biomagnified through food chains. The illness, which came to be known as Minamata disease, was caused by mercury poisoning because of eating contaminated fish. Mercury has very high tendency for binding to proteins and it mainly affects the renal or nervous systems [13] which causes embryocidal, cytochemical and histopathological effects [14]. From the above considerations, it is evident that removal of mercury ions from water and wastewater is very important. Therefore, considerable research efforts by numerous investigators were focused on the removal of mercury compounds by various techniques.

Nowadays, new techniques are focused on adsorption processes because they are more economical than other previously employed such as precipitation,

*Corresponding author.

ultra-filtration and reverse osmosis [15–17]. The mentioned methods usually involve expensive materials and high operation costs; moreover, the application of other methods such as electrodialysis, membrane electrolysis and electrochemical precipitation has been limited due to the high-energy consumption [18]. Beside, ion-exchange process as a cost-effective method, normally involves low-cost materials and convenient operations, and proved to be very effective for removing contaminants from aqua's media [19–21].

Zeolite is well known as a microporous material that its structure is based on an infinitely extending three-dimensional network of AlO_4 and SiO_4 tetrahedral linked to each other by sharing all the oxygen ions. The partial substitution of Si^{4+} by Al^{3+} in the structure of zeolite results in an excess of negative charge which cause cation exchange ability hence, it used to adsorb and remove metal cations, radionuclides as well as ammoniacal nitrogen from municipal wastewaters and electroplating effluents [22–24]. The advantage of zeolite over resins, apart from their much lower cost, is their ion selectivity [25]. Owing to zeolite structural characteristics and their adsorbent properties, they have been applied as chemical sieve, water softener and adsorbents [26]. In recent years, nanosized zeolites have attracted considerable attention as heterogeneous catalysts and adsorbents because of their potential advantages such as shape selectivity of micropores, acid catalytic activity and thermal/hydrothermal stability. In comparison with natural zeolite, the nanosized zeolite could bring better performance due to a high accessibility of active phase and high-external surface area. Studies on heavy metal removal by natural (clinoptilolite) and synthetic (NaP_1) zeolites indicated that the adsorption capacity of synthetic NaP_1 zeolite was ten times greater than the natural zeolite [27,28]. On this aspect, the use of synthetic nano zeolite is a workaround and an improvement for removal of heavy metals hence, in this research, two types of nanozeolite i.e. NaA and ZSM-5 were synthesized and used as an adsorbent for removal of mercury(II) from water solution. Effect of time, temperature and other effective parameter on adsorption procedure was investigated. Finally, the performances of these sorbents were compared with each other.

2. Experimental

2.1. Materials

All reagents used in this work are of analytical grade that supplied from Merck company (Darmstadt, Germany). Working solutions of mercury(II), 1,000 mg L^{-1}, were prepared from mercury(II) chloride salt (CAS number: 7487-94-7). pH adjustments were performed with 0.1 mol L^{-1} of sodium hydroxide and HCl solutions. Tetraethylorthosilicate (TEOS) (CAS number: 78-10-4) and $Al(NO_3)_3$-$9H_2O$ (CAS number: 7784-27-2) were used as Si and Al sources for synthesise of nanozeolites, respectively. Tetrapropylammonium hydroxide (TPAOH) (40 wt.%, CAS number: 2052-49-5) was used as template and surfactant source. 2-mercapto benzo thiazol (MBT) (CAS number: 149-30-4) was used as a chelating agent for determination of mercury(II).

2.2. Instruments

A digital pH meter (model 692, metrohm, Herisau, Switzerland) was used for the pH adjustment. Separation was assisted using a refrigerated centrifuge (Hettich, Universal 320 R). A Lambda-25 UV VIS spectrophotometer was used for determination of mercury (II). The Crystallinity of nanozeolites was examined by powder X-ray diffraction analysis which was carried out on a Phillips powder diffractometer X' Pert MPD using ,PW3123/00 curved Cu-filtered Cu-Ka ($\lambda = 1.540589$ Å) radiation in 2θ range of 2–50°. Fourier transform infrared spectra (FT-IR) were measured with Equinox 55 Bruker with ATR method over the wavelength range of 400–4,000 cm^{-1}. Surface morphology analysis of the adsorbents was carried out using the field emission scanning electron microscope, model S-4160.

2.3. Synthesis of nanozeolites

In order to synthesize ZSM-5 nanozeolite, appropriate amount of aluminum nitrate was added slowly to TPAOH solution with stirring, followed by consecutive addition of distilled water. TEOS, as an organic silica source, which is supposed to come in the aqueous phase slowly was added drop wise during 2 h. The components were mixed with constant stirring then, the mixture aged for 30 min by microwave oven to hydrolyze which results in a concentrated gel. The obtained gel was then charged into Teflon-lined stainless steel autoclaves and crystallized by hydrothermal treatment at 180°C for 48 h without stirring. After this procedure, the product was separated by centrifuge (5,000 rpm), washed several times with distilled water, dried overnight at 120°C and calcinated at 500°C for 5 h in air. The molar composition of ZSM-5 can be expressed as:

$$30\,SiO_2 : 1\,Al_2O_3 : 7.752\,TPAOH : 486.027\,H_2O$$

For preparation of NaA nanozeolite, 1.35 g of sodium aluminate and TEOS was dissolved separately in 25 mL of NaOH solution (6 mol L^{-1}), then aluminate solution was added to silicate along with vigorous shaking. The prepared gel was heated at 40°C for 18 h after formation of solid mass, it was filtered with filter paper, washed several time with distilled water and dried overnight at 80°C then stored until being used. The molar composition of prepared zeolite include:

$$1.85\,SiO_2,\ 1\,Al_2O_3,\ 6\,NaOH,\ 200\,H_2O$$

2.4. Adsorption procedure

In order to perform ion-exchange process for mercury(II) removal, various amounts of target ions (5–50 mg L^{-1}) were placed in a 50 mL flask, 0.05 g of nanozeolite was added and the solution stirred at 500 rpm under optimum conditions (pH 8 and contact time = 60 min), then the liquid was separated from nanozeolites by centrifuging at 5,000 rpm after 3 min. For determination of mercury(II) concentrations, 2 mL of residual solution was mixed with 0.3 mL of MBT (10^{-3} M) and 1 mL of CTAB solution (0.01%), then was made up to 10 mL with borax buffer (0.025 M and pH 10), after 30 min the absorption of complex was measured with UV VIS spectrometer.

3. Results and discussion

3.1. Characterization of nanozeolites

According to Fig. 1 that exhibits the SEM images of the zeolite nanocrystals employed in this paper, the mean sizes of zeolites are 60–80 nm. Fig. 1(a) is the SEM image of ZSM-5 and display that this sample has good monodispersity in comparison with NaA particles (Fig. 1(b)) but NaA nanozeolite exhibit more regular spherical morphology.

The obtained FT-IR spectra in the region of framework vibrations are shown in Fig. 2. The peak around 460 cm^{-1} is assigned to the bending vibrations of aluminosilicate species (Al–O−Si and Si–O−Si tetrahedral). The band at 800–900 cm^{-1} is attributed to the vibration of quartz and Al–OH group. The bending vibration and stretching vibration of Si–O and Si–O–Si can be depicted at 1,060 and 1,115 cm^{-1}, respectively.

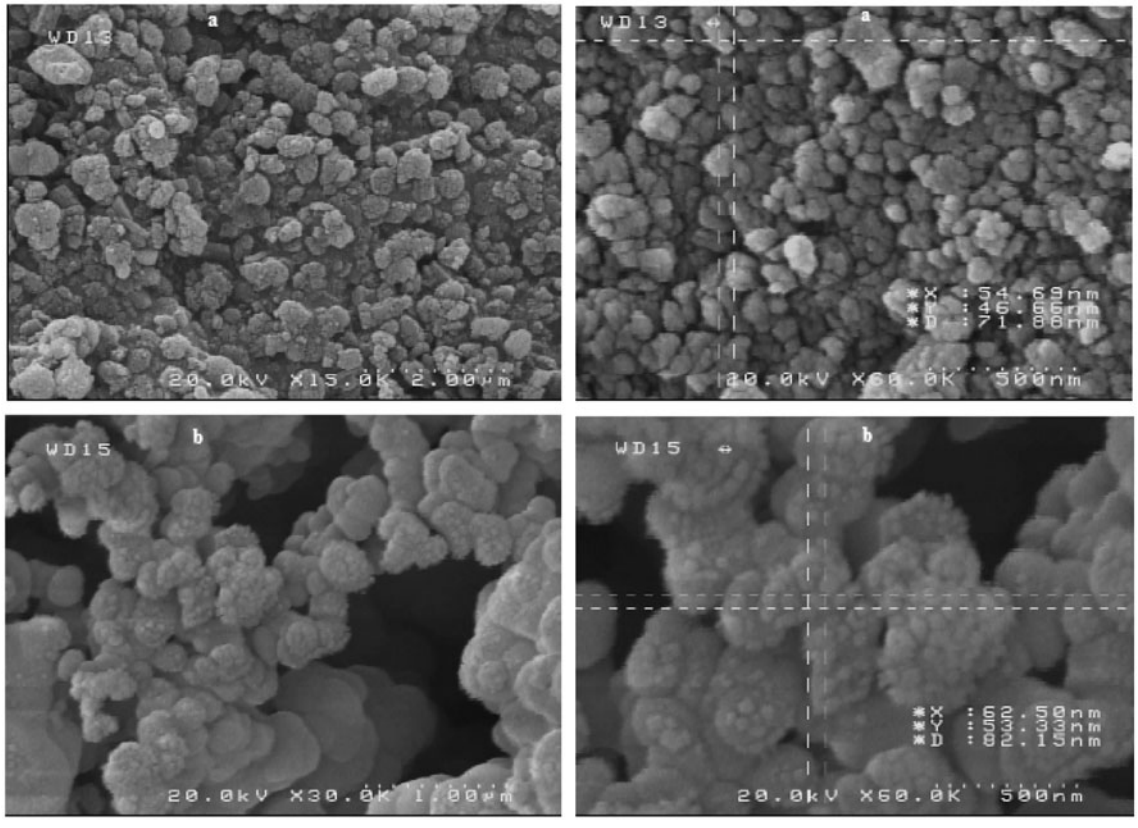

Fig. 1. A typical SEM images for ZSM-5 (a) and NaA (b).

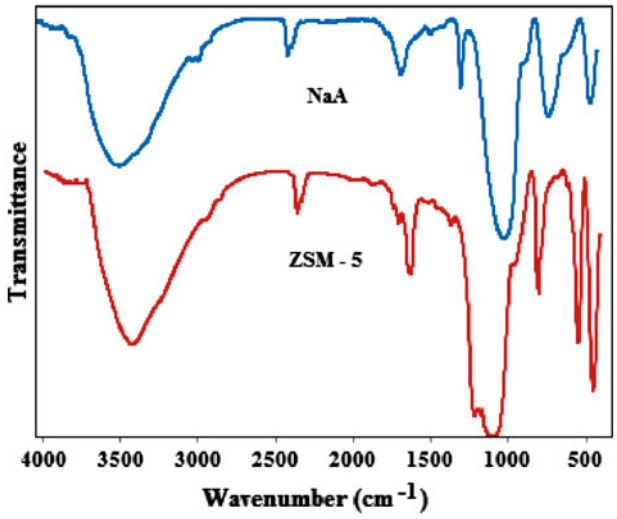

Fig. 2. FT-IR spectrum for nanozeolites.

Furthermore, the bands at 3,000–3,600 cm^{-1} and 1,600 cm^{-1} are corresponding to lattice hydroxyls OH stretching mode, H–OH stretching vibration of free H_2O and water crystallization bending vibration onto the zeolite structure, respectively.

Fig. 3 shows XRD patterns of the prepared NaA and ZSM-5 nanozeolites. The two types of zeolites have a good crystalline degree and observed phases are in good agreement with those reported in the literature [29–31]. The average crystallite size was calculated using Sherrer's equation:

$$D = B\lambda/\beta_{1/2}\cos\theta \quad (1)$$

where D is the average crystallite size of the phase under investigation, B is the Sherrer's constant (0.89), λ is the wavelength of the X-ray beam used (1.54056 Å), $\beta_{1/2}$ is the full width at half maximum of the diffraction peak and θ is the diffraction angle. According to the XRD pattern, the average crystallite size of 75.8 and 68.3 nm was determined for NaA and ZSM-5 nanozeolite, respectively, that is in good agreement with the result of the SEM image.

3.2. Effect of pH

The pH of the solution is one of the most important factors controlling the limit of extractability of metal ions. The effect of pH on sorption was studied by batch method at pH 2–10, keeping the other variables constant. About 0.05 g of the adsorbent was suspended in 50 mL of solution which contain 50 mg L^{-1} of mercury(II) at several pH values. These samples were stirred for 60 min at 150 rpm. Then the samples were centrifuged at 5,000 rpm for 3 min at room temperature to separate the adsorbent. Amount of mercury ions in the solution was determined and the removal percent was calculated with Eq. (2):

$$\%R = (C_0 - C_e)/C_0 \quad (2)$$

where C_0 and C_e are the initial and equilibrium concentrations (mg L^{-1}) of mercury(II) in the solution. The results are depicted in Fig. 4. The optimum pH value at which the maximum removal could be achieved was 8.0. This may be explained by the adsorption surface becoming less positive as the pH value increases therefore, the attraction between mercury(II) and nanozeolite can be increased. The adsorption mechanism for mercury(II) adsorption onto the nanozeolite surface can be expressed as follow (Eqs. (3)–(6)):

$$n\mathrm{MOH}^{+} + \mathrm{M(zeolite)} \leftrightarrow \mathrm{Mn(z)} + \mathrm{M}^{n+} + n\mathrm{OH}^{-} \quad (3)$$

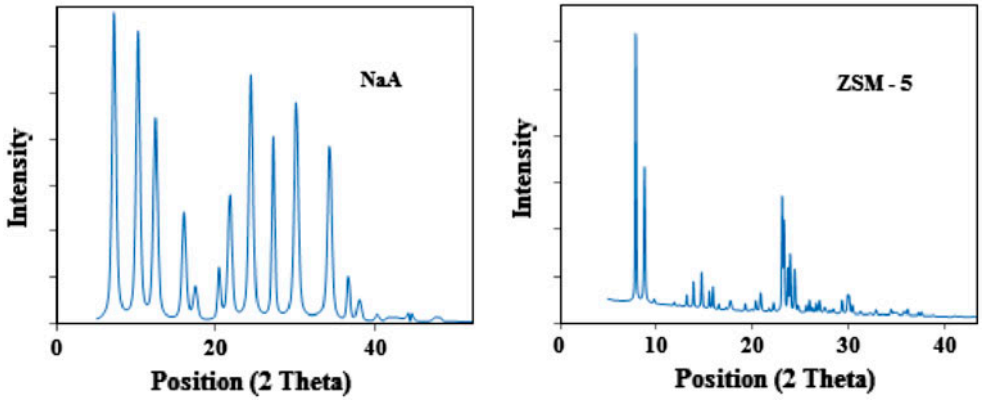

Fig. 3. The XRD pattern for NaA and ZSM nanozeolites.

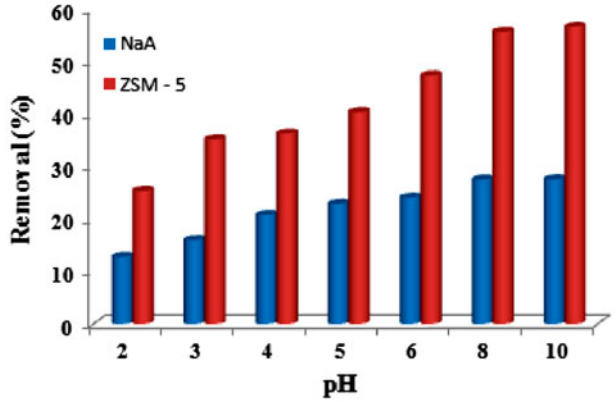

Fig. 4. Effect of pH on mercury(II) removal, conditions; sorbent 0.05 g, amount of analyte 50 mg L^{-1} and time 60 min.

$$n\text{Si–OH} + M^{n+} \leftrightarrow (\text{Si–O})_n\text{–M} + n\text{H}^+ \quad (4)$$

$$\text{SiO–} + \text{MOH}^+ \rightarrow \text{SiOMOH} \quad (5)$$

$$n\text{SiO–} + M^{n+} \leftrightarrow (\text{Si–O})_n\text{–M} \quad (6)$$

The main mechanism for mercury(II) adsorption include: formation of inner sphere complex on the zeolite surface with Si–O group, ion exchange of hydrolyzed divalent metal cation (MOH^+) in aqueous solution and metal cation (mostly Na^+ or Ca^{2+}) in the zeolite framework (Eqs. (3) and (4)), electrostatic interaction and hydrogen bonding. Ion–dipole interaction and hydrophobic interaction can also be considered as adsorption mechanism but the two mentioned mechanisms i.e. ion exchange and complex formation are more responsible for adsorption process.

3.3. Kinetics of adsorption

In order to investigate the effect of contact time between adsorbate and adsorbent on removal efficiency, the time was varied from 5 to 120 min for removal of mercury(II) at three level (12.5, 25 and 50 mg L^{-1}). Removal percent increased rapidly in the first 20 min and then, slowed down as equilibrium was approached (Fig. 5). The increase in adsorption was not significant after 60 min. At this point, the amount of mercury(II) being sorbed by the sorbent was in a state of dynamic equilibrium with the amount of mercury desorbed from the sorbent. Therefore, a time of 60 min was selected for further works. The high-initial uptake rate may be due to the availability of a large number of adsorption sites. As the sites are gradually filled up, adsorption becomes slow and the kinetics will be more dependent on the rate at which the analyte is transported from the bulk phase to the actual adsorption sites.

The kinetic of adsorption can be expressed as the integrated linear form of pseudo-first order and pseudo-second-order kinetic rate equations for the boundary conditions (Eqs. (7) and (8)):

$$\log(Q_e - Q_t) = \log Q_e - k_1 t \quad (7)$$

$$t/Q_t = 1/(k_2 Q_e^2) + (1/Q_e)\, t \quad (8)$$

where k_1 is the pseudo-first-order adsorption rate constant and Q_e, Q_t are the values of the amount adsorbed per unit mass at equilibrium and at any time t and k_2 is the second-order rate constant [32]. Lagergren plot of $\log(Q_e - Q_t)$ vs. t (Fig. 6) in the presence of ZSM-5 and three level of mercury(II) is approximately linear ($R^2 = 0.93$–0.95) although this plot showed better linearity (0.95–0.99) in the presence of

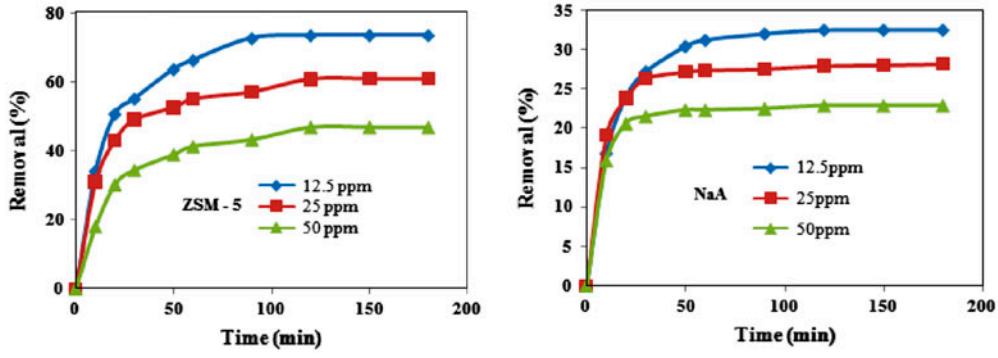

Fig. 5. Effect of contact time for mercury(II) adsorption in three level of target ion.

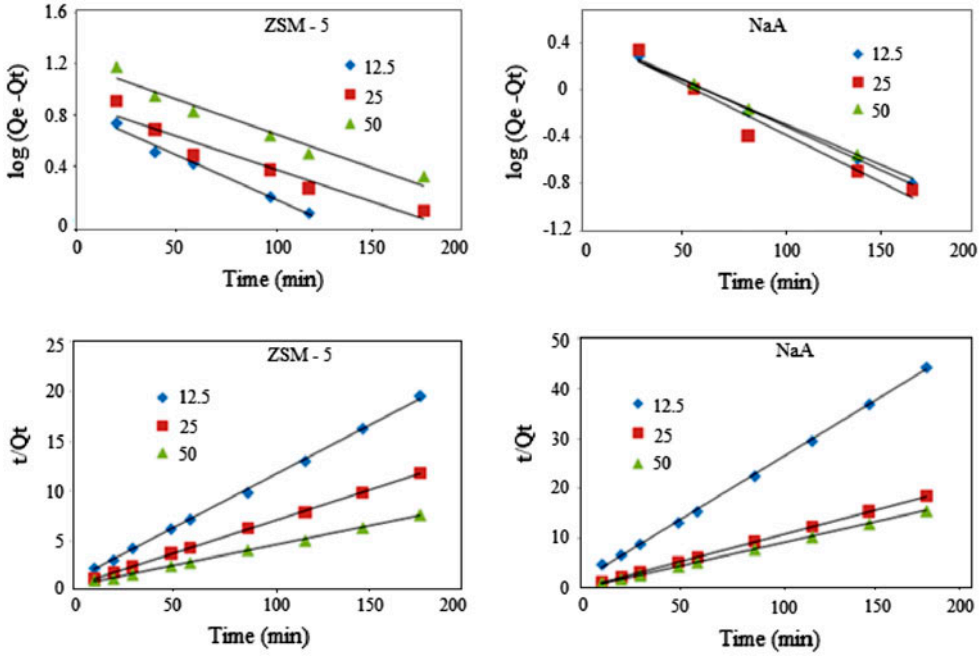

Fig. 6. First and second order kinetic plots for mercury(II) removal.

NaA, but linearity alone does not establish a first-order mechanism. The high differences between the experimental Q_e values and those obtained from Lagergren plots lead to almost total rejection of the first order kinetics. The second-order plots of t/Q_t vs. t (Fig. 6) showed better linearity ($R^2 = 0.999$) for both nanozeolites. The low differences among the experimental Q_e and those obtained from Lagergren plots establish the second-order kinetic (Table 1).

Since, neither the pseudo-first-order nor the pseudo-second-order models can identify the diffusion mechanism, the kinetic results were analyzed by the intraparticle diffusion model. Due to the vigorous agitation of particles during the sorption period, it is assumed that the rate is not limited by mass transfer from the bulk liquid to the particle external surface. The rate-limiting step may be film or intraparticle diffusion [33]. The intraparticle diffusion is governed by the equation:

$$Q_t = k_i t^{0.5} \tag{9}$$

Plot of Q_t vs. $t^{0.5}$ (Fig. 7) at initial concentration of 12.5 mg L^{-1} is approximately linear for NaA ($R^2 = 0.89$) and has good linearity for ZSM-5 ($R^2 = 0.996$). It can also be observed that the plots have intercepts of 2.24 and 3.85 mg g^{-1} for NaA and ZSM-5, respectively. This is indicative of some degree of boundary layer control

Table 1
First-order rate ($\times 10^{-2}$ min^{-1}) and second-order rate ($\times 10^{-2}$ g mg^{-1} min^{-1}) constant and experimental—computed Q_e values from Lagergren and second-order plots at 303 K

		First order			Second order			
	Concentration (mg g^{-1})	K_1	R^2	Q_e (mg g^{-1})	K_2	R^2	Q_e (mg g^{-1})	Q_e (mg g^{-1}) Experimental
	12.5	2.1	0.997	1.049	3.0	0.999	4.29	3.9
NaA	25	2.3	0.956	1.054	2.6	0.999	10.0	6.86
	50	2.0	0.999	1.047	2.8	0.999	11.76	11.2
	12.5	1.9	0.948	8.7	0.83	0.999	10.0	9.2
ZSM-5	25	1.0	0.931	7.07	0.57	0.999	16.38	15.2
	50	1.1	0.956	14.68	0.23	0.999	26.31	23.4

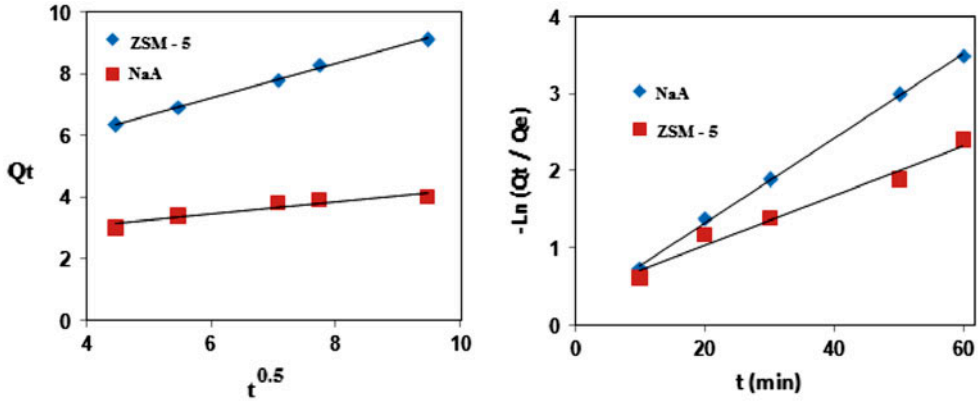

Fig. 7. Plot of intra-particle diffusion and liquid film diffusion for mercury(II) ions adsorbed on nanozeolites.

and further shows that the intraparticle diffusion is not the only rate-limiting step. The values of the intercept also indicated that with larger the intercept the greater is the boundary layer effect.

The liquid film diffusion model, which explains the role of transport of the adsorbate from the liquid phase up to the solid phase boundary, can be expressed as:

$$\ln(1-F) = -k_{fd}\,t \tag{10}$$

where F is the fractional attainment of equilibrium ($F = Q_t/Q_e$) and k_{fd} is the adsorption rate constant. Plotting $-\ln(1-F)$ vs. t (Fig. 7) produced linear curve ($R^2 = 0.97$–0.99) for two type of zeolites but with non-zero intercept (0.2–0.3) against the predictions of the model. The small intercepts might point out limited applicability of the model and thus, indicating a role for liquid phase transports of the mercury(II) to the sorbent surface in controlling the kinetics. This result revealed that the sorption mechanism is a complicated process with more than one mechanisms involved which is related to the active groups of sorbent.

3.4. Effect of mercury(II) concentration and isotherm studies

The removal efficiency by ZSM-5 and NaA in different concentration of mercury(II) is depicted in Table 2. Decrease in uptake efficiency with increase in initial concentration is due to the fact that sorption sites took up the available metal ions more quickly at low concentration, but metal needed to diffuse to the inner sites of the sorbent for high concentration. Moreover, as the metal/sorbent ratio increases, sorption sites are saturated, resulting in decreases in the sorption efficiency. Additionally, it was noticed that an increase in initial metal concentration leads to an increase in the sorption capacity of mercury by nanozeolites. This is a result of the increase in the driving force the concentration gradient, as an increase in the initial mercury concentrations.

The equilibrium adsorption isotherm is important for designing an adsorption system because these models can describe the interactive behaviour of the solution and the adsorbent. Hence the effect of mercury(II) concentrations on adsorption process was analyzed in terms of Langmuir, Freundlich and Temkin isotherms and the results are depicted in Table 3. The Langmuir model can be expressed as:

$$C_e/Q_e = 1/(Q_m b) + C_e/Q_m \tag{11}$$

where Q_e is the amount of metal ions sorbed per unit mass of the sorbent (mg g^{-1}) and C_e the amount of metal ions in the liquid phase at equilibrium (mg L^{-1}). The Q_m is maximum adsorption capacity and b is the Langmuir coefficient. Three assumes of this model include: (i) presence of identical sites which are energetically uniform on the solid surface, (ii) there is no interactions between adsorbed species, meaning that

Table 2
Removal efficiency in different concentrations of mercury(II)

Concentration (mg L^{-1})	Removal (%)	
	NaA	ZSM-5
12.5	34	73
25	28	60
50	10	46

Table 3
Isotherm models data for mercury adsorption

Adsorption isotherms	Isotherms constant	Values (NaA)	Values (ZSM-5)
Langmuir	Q_m (mg g^{-1})	32.25	45.4
	b (L mg^{-1})	0.061	0.054
	R_L	0.17–0.56	0.17–0.60
	R^2	0.971	0.944
Freundlich	K_f (mg$^{1-1/n}$ g^{-1}) (L)$^{1/n}$	1.054	5.09
	n	1.46	2.08
	R^2	0.999	0.996
Temkin	K_T (L mg^{-1})	0.19	0.63
	B_1 (mg g^{-1})	6.25	9.056
	R^2	0.966	0.941

the amount adsorbed has no influence on the rate of adsorption and (iii) formation of a monolayer in saturation state [34,35]. So, this model is based on the assumption of structurally homogeneous sorbent where all the sorption sites are energetically the same and identical. The essential characteristics of the Langmuir isotherm can be explained in terms of a dimensionless constant separation factor (R_L), calculated by use of the equation:

$$R_L = 1/(1 + bC_i) \tag{12}$$

where C_i is the initial concentration of metal ions. R_L describes the type of Langmuir isotherm, to be irreversible ($R_L = 0$), favourable ($0 < R_L < 1$), linear ($R_L = 1$) or unfavourable ($R_L > 1$) [36]. The Langmuir plots have been depicted in Fig. 8 and indicated that the curve for adsorption of mercury onto NaA has better linearity in comparison with ZSM-5. Although R_L value (0.17–0.60) indicate favourable sorption of mercury(II) ions on these sorbents.

The Freundlich model that suggests the adsorption–complexation reactions in the adsorption process is represented as:

$$Q_e = K_f C_e^{1/n} \tag{13}$$

where n and K_f are the Freundlich coefficients which evaluated from the slopes and intercepts of linear plot.

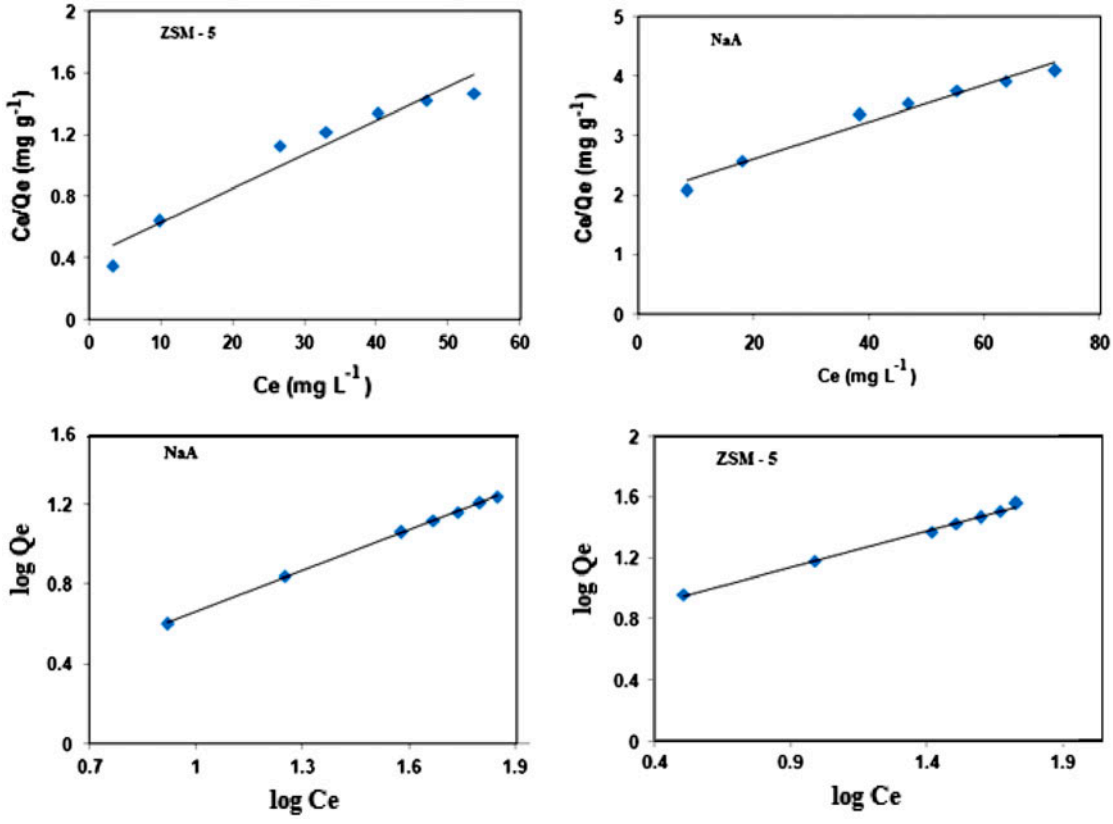

Fig. 8. Langmuir and Freundlich isotherm models for the adsorption of mercury(II) ions.

The magnitude of the Freundlich constant, n, gives a measure of favourability of adsorption. The values of n between 1 and 10 (i.e. $1/n < 1$) represents a favorable sorption [37]. The Freundlich isotherm (Fig. 8) is linear if $1/n = 1$ and as $1/n$ decreases, the isotherm becomes more non-linear. Amount of n is equal to 1.46 and 2.08 for NaA and ZSM-5, respectively, which indicates the sorption process, is favourable. The correlation coefficient value of Freundlich isotherm was higher as compared with Langmuir model and lead to the conclusion that the complexation reactions also are the adsorption mechanism for removal of mercury(II) with nanozeolites.

The Temkin isotherm takes into account the interactions between adsorbents and metal ions to be adsorbed and is based on the assumption that the free energy of adsorption is a function of the surface coverage. The isotherm model is written as:

$$Q_e = B_1 \ln K_T + B_1 \ln C_e \tag{14}$$

the Temkin isotherm constants K_T and B_1 are calculated by plot of Q_e vs. $\ln C_e$ (Fig. 9). The correlation coefficient value of this model is approximately near to the Langmuir model ($R^2 = 0.94$–0.96), which indicates that the heat of sorption for all the sorbate molecules on the surface layer of sorbents decreases linearly due to the sorbent–sorbate interactions. Therefore, the above two systems can be characterized by uniform distribution of binding energies.

3.5. Thermodynamic studies

The value of Q_e increased with raising the temperature from 298 to 335 K suggesting endothermic interactions. These results indicate that mercury(II) move towards solid phase from the solution with the rise in temperature, and the excess energy supply promotes adsorption. The thermodynamic parameters for the adsorption process, ΔH (kJ mol^{-1}), ΔS (JK^{-1} mol^{-1}) and ΔG (kJ mol^{-1}), could be evaluated using the equations:

$$\Delta G = -RT \ln K_d \tag{15}$$

$$\Delta G = \Delta H - T\Delta S \tag{16}$$

$$\ln K_d = \Delta S/R - \Delta H/RT \tag{17}$$

where K_d, R and T are the distribution coefficient of the adsorbate (Q_e/C_e), gas constant (8.314×10^{-3} kJK^{-1} mol^{-1}) and absolute temperature (K), respectively [38]. The plot of ln K_d vs. $1/T$ is linear with the slope and the intercept giving values of ΔH and ΔS. Mercury(II)–ZSM-5 interaction exhibits negative values of Gibbs free energy (Table 4) indicated that the adsorption process is spontaneous. Although mercury(II)–NaA interaction is non-spontaneous but increasing in ΔS value can promote the adsorption of mercury(II) by nanozeolites hence, mercury(II)–zeolites adsorption reaction can be entropy stabilized.

3.6. Comparison of nanozeolites performance

In this research, two types of nanozeolites have been synthesized and used for removal of mercury(II) from aqua's media. The results indicated that ZSM-5 has better performance with respect to NaA zeolite. The removal efficiency with ZSM-5 is 40–70% but the removal value with NaA is 10–35%. Moreover, the maximum Langmuir monolayer capacity for ZSM is 30% higher than the Q_m value for NaA hence, ZSM can be utilized for treatment of higher amount of mercury(II) in comparison with NaA zeolite. The other point about the two type nanozeolites is their

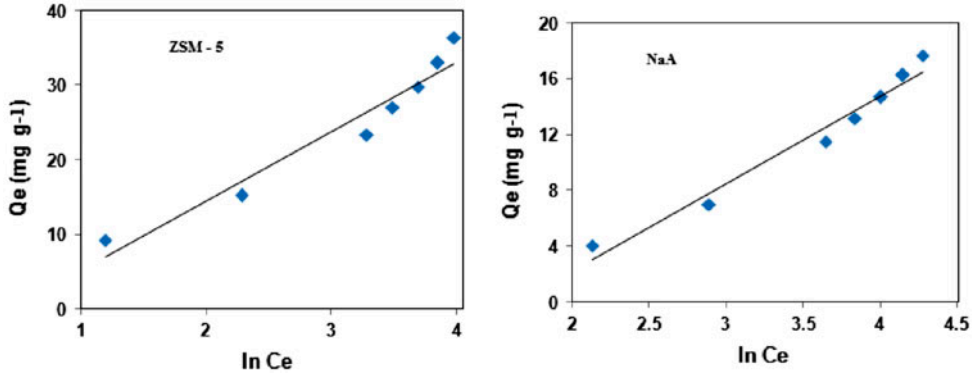

Fig. 9. Temkin models plot for mercury(II) removal.

Table 4
Thermodynamic data for adsorption of mercury(II) (adsorbent 1.0 g L^{-1}, mercury(II) 25 mg L^{-1}, pH 8.0 and time 60 min)

	ΔH (kJ mol^{-1})	ΔS (JK^{-1} mol^{-1})	ΔG (kJ mol^{-1})		
			298 K	313 K	333 K
ZSM-5	+30.69	+104.5	−0.3	−1.86	−3.94
NaA	+12.58	+33.26	+2.74	+2.25	+1.59

thermodynamic behaviour. The ΔS value of ZSM is more positive with respect to NaA that can promote the adsorption of mercury(II) with ZSM nanozeolite. Although negative values of Gibbs free energy for ZSM indicated that the adsorption process is spontaneous. But this parameter for NaA is positive and the process is non-spontaneous. Two reasons can be expressed for better performances of ZSM nanozeolite. According to molar composition of nanozeolites, there is more silanol groups in the structure of ZSM (30 SiO_2) which cause the presence of more adsorption sites in the surface of sorbent. Moreover, the SEM images indicated that ZSM nanozeolite has more monodispersity in comparison with NaA zeolite. This characteristic can help the ZSM particles to be more dispersive in aqua's media. Beside, with more monodispersity the functional groups can be more accessible in order to interact with mercury(II) ions.

3.7. Comparison with other methods

The equilibrium time and calculated sorption capacity (Q_m) of nanozeolites tested in the present study and other sorbents, which have been reported in the literature for mercury(II) removal, present in Table 5. It is obvious that the performance of the prepared sorbents was good with respect to removal efficiency and demonstrate satisfactory sorption capacity which is compatible with the values found in the literature. Nanozeolite appears to be a promising sorbent for the removal of mercury from aquatic systems due to its preparation which is simple and has low cost when compared with different available sorbents.

3.8. Cost comparison of zeolite with common adsorbents

When the prices of a number of common adsorbents are compared, as shown in Table 6, zeolite appear to be the cheapest being in the same range as clay and perlite. Some cost addition will of course be required if any treatment like acid or base activation is to be done. These data indicate that nanozeolite is a good candidate for heavy metal adsorption because of low cost, easy to preparation and green characteristic.

Table 5
Comparison of presented method with the literature for mercury(II) removal

Sorbent	Q_{max} (mg g^{-1})	Time (min)	Refs.
Malt spent rootlets	50	24 h	[1]
[a]PHM-N-methacryloyl-(l)-cysteine-IIP	0.45	10	[4]
[b]TAR-methacrylic acid-IIP	25	20	[5]
2-mercaptoethylamine-IIP	28	50	[6]
Mesoporous aluminosilicate sieve	20.65	100	[7]
Thiol-functionalized zeolite	89	24 h	[8]
Fe_3O_4@SiO_2–SH	148.8	4 h	[10]
Thio-modified cellulose resins	23	10	[11]
Biomass of *Sargassum glaucescens*	147	90	[12]
Eucalyptus bark	33.11	30	[13]
Sulfur-functionalized silica	24 h	47.5	[21]
Sheep bone charcoal	12.5	120	[35]
NaA	32.25	60	–
ZSM-5	45.4	60	–

[a]Poly(hydroxyethyl methacrylate)-ion imprinted polymer.
[b]4-(2-Thiazolylazo) resorcinol.

Table 6
Cost comparison of zeolite with common adsorbents

Types of adsorbent	Price (US $ kg^{-1})
Clay	0.24–1.04
Commercial activated carbon	20–22
Chitosan	11–50
Zeolite	0.1–3
Perlite	0.05–1.5
Fe_3O_4	500–1,000
MWCNT	4,000–50,000
Lignin	0.25–2
Cellulose powder, microcrystalline	80–300

4. Conclusion

In the present study, crystalline nano ZSM-5 and NaA zeolites were synthesized and used for removal of mercury(II). The different factors influencing the uptake efficiency of mercury(II) were investigated. Mercury(II)–zeolite interactions were accompanied by increasing in ΔS and ΔH value and the adsorption process was spontaneous for ZSM-5 and non-spontaneous for NaA. Moreover, optimum contact time was 60 min with both zeolite types and kinetic of the interaction have been described by pseudo-second-order mechanism. The performance of this method was in good level with respect to removal efficiency and adsorption capacity. Moreover, nanozeolite can

transfer mercury(II) contamination problem of high-volume samples to a few amount of easily handled solid in order to reduce its hazardous impact on ecosystem.

References

[1] V.A. Anagnostopoulos, I.D. Manariotis, H.K. Karapanagioti, C.V. Chrysikopoulos, Removal of mercury from aqueous solutions by malt spent rootlets, Chem. Eng. J. 213 (2012) 135–141.

[2] A. Hutchison, D. Atwood, Q.E. Santilliann-Jiminez, The removal of mercury from water by open chain ligands containing multiple sulfurs, J. Hazard. Mater. 156 (2008) 458–465.

[3] P. Zhao, X. Guo, C. Zheng, Removal of elemental mercury by iodine-modified rice husk ash sorbents, J. Environ. Sci. 22 (2010) 1629–1636.

[4] M. Andaç, S. Mirel, S. Şenel, R. Say, A. Ersöz, A. Denizli, Ion-imprinted beads for molecular recognition based mercury removal from human serum, Int. J. Biol. Macromol. 40 (2007) 159–166.

[5] D.K. Singh, S. Mishra, Synthesis and characterization of Hg(II)-ion-imprinted polymer: Kinetic and isotherm studies, Desalination 257 (2010) 177–183.

[6] M. Firouzzare, Q. Wang, Synthesis and characterization of a high selective mercury(II)-imprinted polymer using novel aminothiol monomer, Talanta 101 (2012) 261–266.

[7] M. Liu, L.A. Hou, B. Xi, Y. Zhao, X. Xia, Synthesis, characterization, and mercury adsorption properties of hybrid mesoporous aluminosilicate sieve prepared with fly ash, Appl. Surf. Sci. 273 (2013) 706–716.

[8] X.-Y. Zhang, Q.-C. Wang, S.-Q. Zhang, X.-J. Sun, Z.-S. Zhang, Stabilization/solidification (S/S) of mercury-contaminated hazardous wastes using thiol-functionalized zeolite and Portland cement, J. Hazard. Mater. 168 (2009) 1575–1580.

[9] A. Chojnacki, K. Chojnacka, J. Hoffmann, H.G. Górecki, The application of natural zeolites for mercury removal: From laboratory tests to industrial scale, Miner. Eng. 17 (2004) 933–937.

[10] S. Zhang, Y. Zhang, J. Liu, Q. Xu, H. Xiao, X. Wang, H. Xu, J. Zhou, Thiol modified Fe_3O_4@SiO_2 as a robust, high effective, and recycling magnetic sorbent for mercury removal, Chem. Eng. J. 226 (2013) 30–38.

[11] Y. Takagai, A. Shibata, S. Kiyokawa, T. Takase, Synthesis and evaluation of different thio-modified cellulose resins for the removal of mercury(II) ion from highly acidic aqueous solutions, J. Colloid Interface Sci. 353 (2011) 593–597.

[12] A. Esmaeili, B. Saremnia, M. Kalantar, Removal of mercury(II) from aqueous solutions by biosorption on the biomass of *Sargassum glaucescens* and *Gracilaria corticata*, Arab. J. Chem. doi: 10.1016/j.arabjc.2012.01.008.

[13] I. Ghodbane, O. Hamdaoui, Removal of mercury(II) from aqueous media using eucalyptus bark: Kinetic and equilibrium studies, J. Hazard. Mater. 160 (2008) 301–309.

[14] P. Miretzky, A.F. Cirelli, Hg(II) removal from water by chitosan and chitosan derivatives: A review, J. Hazard. Mater. 167 (2009) 10–23.

[15] J. Jiménez-Jiménez, M. Algarra, E. Rodríguez-Castellón, A. Jiménez-López, J.C.G. Esteves da Silva, Hybrid porous phosphate heterostructures as adsorbents of Hg(II) and Ni(II) from industrial sewage, J. Hazard. Mater. 190 (2011) 694–699.

[16] G. Zolfaghari, A. Esmaili-Sari, M. Anbia, H. Younesi Taguchi, Optimization approach for Pb(II) and Hg(II) removal from aqueous solutions using modified mesoporous carbon, J. Hazard. Mater. 192 (2011) 1046–1055.

[17] A. Dąbrowski, Z. Hubicki, P. Podkościelny, E. Robens, Selective removal of the heavy metal ions from waters and industrial wastewaters by ion-exchange method, Chemosphere 56 (2004) 91–106.

[18] T.A. Kurniawan, G.Y.S. Chan, W.H. Lo, S. Babel, Physico–chemical treatment techniques for wastewater laden with heavy metals, Chem. Eng. J. 118 (2006) 83–98.

[19] K.S. Hui, C.Y.H. Chao, S.C. Kot, Removal of mixed heavy metal ions in wastewater by zeolite 4A and residual products from recycled coal fly ash, J. Hazard. Mater. 127 (2005) 89–101.

[20] W. Qiu, Y. Zheng, Removal of lead, copper, nickel, cobalt, and zinc from water by a cancrinite-type zeolite synthesized from fly ash, Chem. Eng. J. 145 (2009) 483–488.

[21] N. Saman, K. Johari, H. Mat, Synthesis and characterization of sulfur-functionalized silica materials towards developing adsorbents for mercury removal from aqueous solutions, Microporous Mesoporous Mater. 194 (2014) 38–45.

[22] R. Egashira, S. Tanabe, H. Habaki, Adsorption of heavy metals in mine wastewater by Mongolian natural zeolite, Proc. Eng. 42 (2012) 49–57.

[23] V. Swarnkar, N. Agrawal, R. Tomar, Sorption of chromate by HDTMA-exchanged zeolites, J. Chem. Pharm. Res. 3 (2011) 520–529.

[24] S.R. Taffarel, J. Rubio, On the removal of Mn^{2+} ions by adsorption onto natural and activated Chilean zeolites, Min. Eng. 22 (2009) 336–343.

[25] G.T. Vuong, V.T. Hoang, D.T. Nguyen, T.O. Do, Synthesis of nanozeolites and nanozeolite-based FCC catalysts, and their catalytic activity in gas oil cracking reaction, Appl. Catal., A 382 (2010) 231–239.

[26] H. Ghobarkar, O. Schäf, U. Guth, Zeolites—From kitchen to space, Prog. Solid State Chem. 27 (1999) 29–73.

[27] E. Alvarez-Ayuso, A. Garcia-Sanchez, X. Querol, Purification of metal electroplating waste waters using zeolites, Water Res. 37 (2003) 4855–4862.

[28] Y. Kang, W. Shan, J. Wu, Y. Zhang, X. Wang, W. Yang, Y. Tang, Uniform nanozeolite microspheres with large secondary pore architecture, Chem. Mater. 18 (2006) 1861–1866.

[29] H.R. Tashauoei, A.H. Movahedian, M. Kamali, M.M. Amin, M. Nikaeen, Removal of hexavalent chromium (VI) from aqueous solutions using surface modified nanozeolite A, Int. J. Environ. Res. 4 (2010) 491–500.

[30] D. Nibou, H. Mekatel, S. Amokrane, M. Barkat, M. Trari, Adsorption of Zn^{2+} ions onto NaA and NaX zeolites: Kinetic, equilibrium and thermodynamic studies, J. Hazard. Mater. 173 (2010) 637–646.

[31] M.M. Mohamed Mokhtar, N.R. Katabathini, S.H. Huda, N.B. Sulaiman, I.H. Abd El-Maksod, Synthesis and characterization of partially crystalline nanosized ZSM-5 zeolites, Ceram. Int. 39 (2013) 683–689.

[32] G. Özdemir, S. Yapar, Adsorption and desorption behavior of copper ions on Na-montmorillonite: Effect of rhamnolipids and pH, J. Hazard. Mater. 166 (2009) 1307–1313.
[33] V.K. Gupta, Deepak Pathania, Shilpi Agarwal, S. Sharma, Removal of Cr(VI) onto *Ficus carica* biosorbent from water, Environ. Sci. Pollut. Res. 20 (2013) 2632–2644.
[34] J. Wang, R. Peng, J. Yang, Y. Liu, X. Hu, Preparation of ethylenediamine-modified magnetic chitosan complex for adsorption of uranyl ions, Carbohydr. Polym. 84 (2011) 1169–1175.
[35] A. Dawlet, D. Talip, H.Y. Mi, M. MaLiKeZhaTi, Removal of mercury from aqueous solution using sheep bone charcoal, Procedia Environ. Sci. 18 (2013) 800–808.
[36] R. Ansari, B. Seyghali, A. Mohammad-khah, M.A. Zanjanchi, Highly efficient adsorption of anionic dyes from aqueous solutions using sawdust modified by cationic surfactant of cetyltrimethylammonium bromide, J. Surfactants Deterg. 15 (2012) 557–565.
[37] B. Shah, C. Mistry, A. Shah, Seizure modeling of Pb(II) and Cd(II) from aqueous solution by chemically modified sugarcane bagasse fly ash: Isotherms, kinetics, and column study, Environ. Sci. Pollut. Res. 20 (2013) 2193–2209.
[38] M.M. Abou-Mesalam, Sorption kinetics of copper, zinc, cadmium and nickel ions on synthesized silicoantimonate ion exchanger, Colloids Surf., A 225 (2003) 85–94.